Earth Planets Space, **52**, 403–413, 2000

Geodetically observed surface displacements of the 1999 Chi-Chi, Taiwan, earthquake

Ming Yang[1], Ruey-Juin Rau[2], Jyh-Yih Yu[1], and Ting-To Yu[2]

[1] *Department of Surveying Engineering, National Cheng Kung University, Tainan, Taiwan*
[2] *Satellite Geoinformatics Research Center, National Cheng Kung University, Tainan, Taiwan*

(Received February 18, 2000; Revised May 17, 2000; Accepted May 18, 2000)

The 21 September 1999 Chi-Chi, Taiwan, earthquake of magnitude $M_W = 7.6$ ($M_L = 7.3$) severely deformed the Earth's crust in the central Taiwan region. The earthquake created an 85-km-long surface rupture along the Chelungpu fault. The epicenter was located at 23.85°N, 120.81°E, near the southern end of the rupture zone. Three-dimensional displacements of 285 geodetic control stations were determined in this study from Global Positioning System (GPS) observations collected before and after the earthquake. The detailed surface displacement field shows that individual stations are vertically uplifted by up to 4 m and displaced horizontally by up to 9 m, with the largest displacement occurring near the northern end of the ruptured thrust fault. The azimuth of the surface displacement field is approximately parallel to the direction of tectonic convergence of the Eurasian and Philippine Sea plates. The maximum three-dimensional displacement of 9.9 m is among the largest fault movements ever measured for modern earthquakes.

1. Introduction

Taiwan lies at the junction of the Eurasian plate and the Philippine Sea plate, which converge near latitude 24°N at ~7 cm/yr in a N50W direction (DeMets *et al.*, 1990; Seno *et al.*, 1993; Yu *et al.*, 1997; Yu *et al.*, 1999). As a result, this region is one of the world's most unstable areas with frequent major earthquakes. The 01:47 local time (17:47 GMT the previous day), 21 September 1999 Chi-Chi earthquake was the largest earthquake ($M_W = 7.6$, $M_L = 7.3$) that struck the island in this century. This massive earthquake not only produced significant horizontal and vertical surface displacements over a very large area of 10000 km^2 (100 km × 100 km), but also caused approximately 10000 collapsed structures in several cities along the ruptured Chelungpu fault, and over 2300 fatalities and 8700 injuries.

In this study, we used Global Positioning System (GPS) geodetic data to quantify the three-dimensional surface displacement pattern associated with the Chi-Chi earthquake. Pre-earthquake data were collected between 1995 and 1998 from global and regional permanent GPS tracking networks, as well as at Taiwan's first- and second-order geodetic control stations. Post-earthquake data were collected within one month of the earthquake, including field surveys at geodetic control points located in the central Taiwan area and continuous observations at stations of the regional GPS tracking network. The resultant high precision co-seismic displacement field of the earthquake can be further exploited to provide valuable information for seismologists and earthquake engineers to study the complex pattern of surface faulting in Taiwan.

2. GPS Data Processing

Since 1990, researchers from Taiwan started to use GPS interferometry to characterize regional tectonic motion and estimate relative velocities near and within the island (Yu *et al.*, 1997; Yu *et al.*, 1999). It is clear in Fig. 1 that significant velocity contrasts are present in the central, south and east regions of the island. In 1995, a decision was made by the Ministry of the Interior, R.O.C. to establish a new geodetic datum, the Taiwan geodetic datum 1997 (TWD97), to replace the old reference frame created in the late 1970s by means of triangulation. The GPS-based TWD97 was directly linked with the International Terrestrial Reference Frame (ITRF) by connecting a regional GPS permanent tracking network with globally distributed International GPS Service (IGS) stations. The regional tracking network was further intensified with 726 first- and second-order geodetic control stations that covered the entire region of Taiwan with an average spacing of 10–15 km, including the island of Taiwan and several islands across Taiwan Strait, adjacent to Mainland China.

In this study, pre-earthquake data were obtained in field surveys between April 1995 and May 1998 and from continuous observations at stations of the regional continuous GPS tracking network and the IGS global network. We divided these data into two groups. The first group contained daily GPS observations made at the global and regional tracking sites. The second group, however, only included measurements collected at the first- and second-order control stations during 124 field sessions, and continuously recorded regional tracking data covering 24 hours on the day of each field session. Forty-eight IGS stations were used in the study. Taiwan's only IGS site, TAIW, located in the northern part of the island, is the only station included in both the global and the regional networks. Figure 2 illustrates the geographical

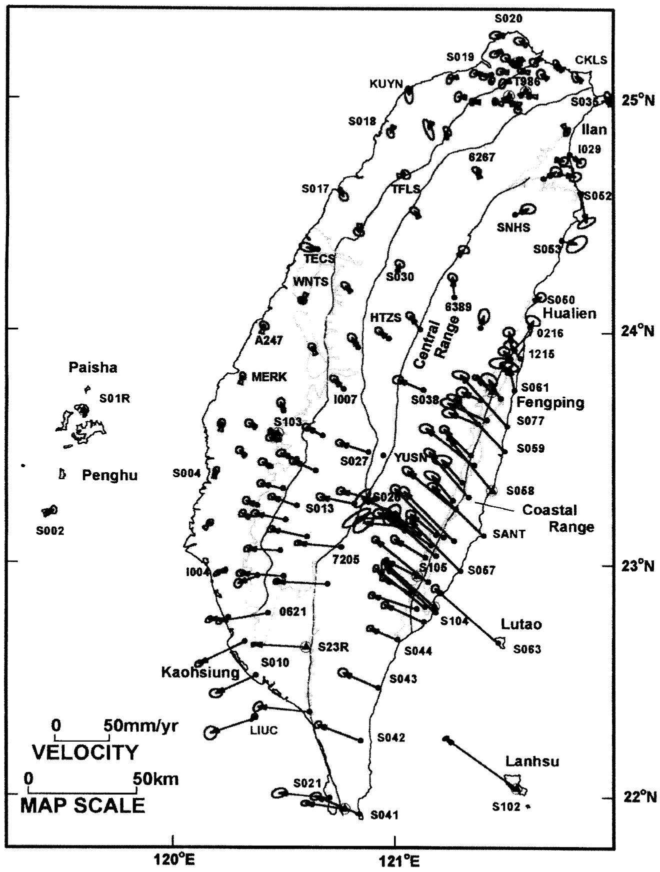

Fig. 1. Taiwan tectonic velocity field after Yu *et al.* (1997).

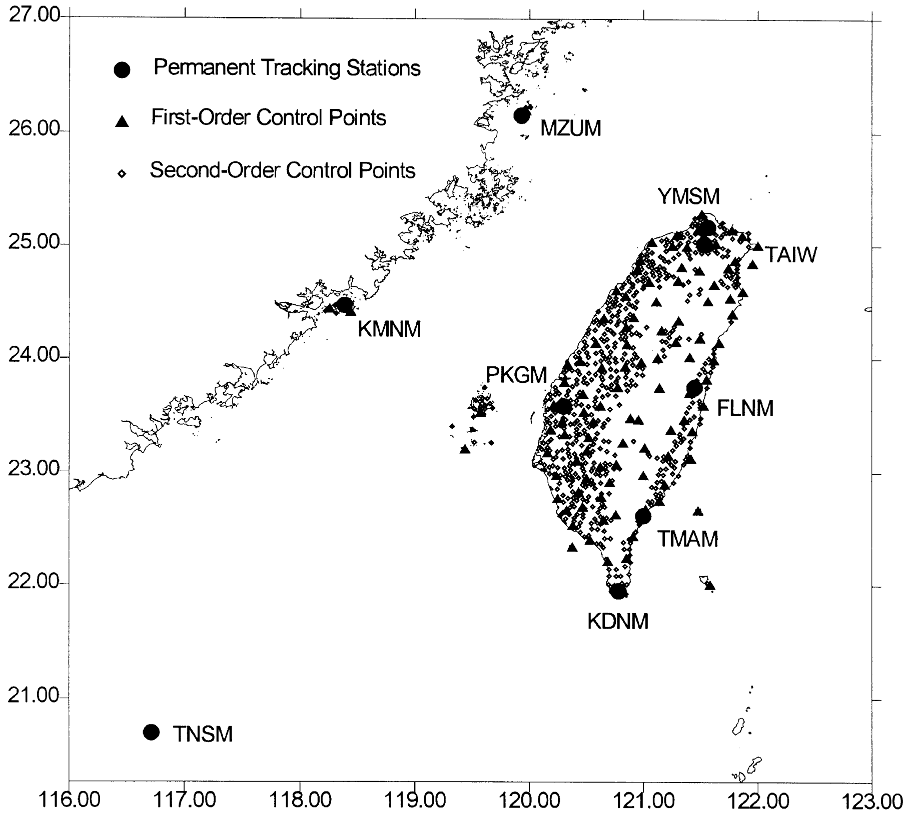

Fig. 2. Spatial distribution of the TWD97 stations, excluding two second-order stations located on Nan-Sa Island in the South China Sea near the Philippines.

Table 1. GPS data reduction summary.

Models	Values
Data intervals	30 sec for tracking data, 15 sec for field survey data
Elevation angle cut-off	15 °
GPS orbit	IGS precise ephemeris
Ionospheric delay	Zero (canceled by forming the ionosphere-free phase)
Tropospheric delay	Modified Hopfield model value with one estimated correction parameter per station every 4 hours
a priori phase sigma	±1 cm
Data editing threshold	3-sigma value

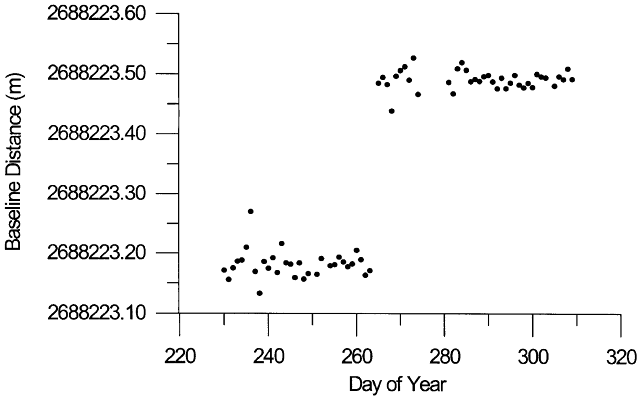

Fig. 3. Daily solutions of baseline distance between IGS site GUAM and tracking station FLNM.

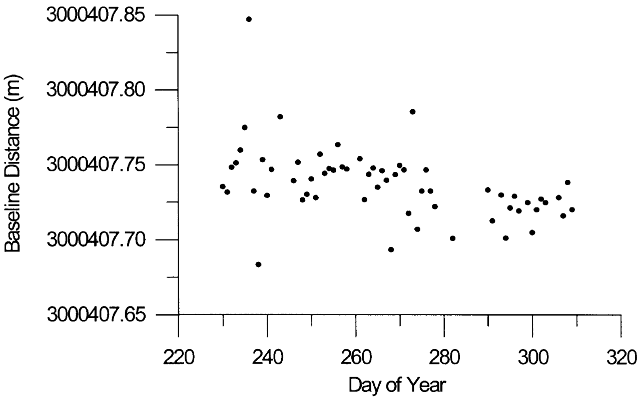

Fig. 4. Daily solutions of baseline distance between IGS site GUAM and tracking station KMNM.

Table 2. ITRF94 epoch 1997.0 velocities and velocity/coordinate standard deviations for the nine regional tracking stations in the north-south (N), east-west (E), and vertical (U) directions.

Station		Velocity (m/yr)	Velocity Sigma (±m/yr)	Coordinate Sigma (±m)
FLNM	N	0.0076	0.0002	0.0003
	E	0.0098	0.0005	0.0007
	U	−0.0179	0.0011	0.0013
KDNM	N	−0.0069	0.0002	0.0003
	E	0.0050	0.0005	0.0007
	U	−0.0170	0.0011	0.0014
KMNM	N	−0.0092	0.0002	0.0003
	E	0.0330	0.0005	0.0008
	U	−0.0181	0.0011	0.0015
MZUM	N	−0.0096	0.0002	0.0003
	E	0.0326	0.0005	0.0008
	U	−0.0216	0.0011	0.0019
PKGM	N	0.0000	0.0002	0.0003
	E	0.0270	0.0005	0.0008
	U	−0.0665	0.0011	0.0015
TAIW	N	−0.0086	0.0002	0.0002
	E	0.0364	0.0005	0.0006
	U	−0.0374	0.0011	0.0014
TMAM	N	0.0021	0.0002	0.0003
	E	0.0028	0.0005	0.0008
	U	−0.0170	0.0011	0.0016
TNSM	N	−0.0063	0.0003	0.0004
	E	0.0358	0.0010	0.0012
	U	−0.0367	0.0024	0.0028
YMSM	N	−0.0103	0.0005	0.0004
	E	0.0352	0.0011	0.0008
	U	−0.0178	0.0011	0.0013

distribution of the TWD97 stations. Installed in the regional tracking network were dual frequency TurboRogue receivers with Dorne & Margolin geodetic antennas. The continuous data were recorded every 30 seconds by the regional tracking network, in accordance with the IGS standard. For the 124 field sessions, the fundamental session length was 4–5 hours, and the dual frequency observations recorded by GPS receivers of various types were sampled every 15 seconds. The number of GPS receivers used in the field surveys varied greatly, with a minimum of 2 and a maximum of 123 stations involved in a single session. As the GPS satellite geometry was different for various sessions, all stations were surveyed with multiple occupations.

During GPS data reduction, a number of physical parameters contained in the double-differenced phase observation equation must either be effectively modeled or estimated together with the unknown station coordinates. Generally these parameters include orbital positions of the GPS satellites, ionospheric and tropospheric delays, and carrier phase integer ambiguities (Beutler *et al.*, 1996; Goad *et al.*, 1996;

Table 3. Three-dimensional displacement vectors and associated sigma values sampled at 285 TWD97 stations.

Station	Long. (°)	Lat. (°)	de (cm)	dn (cm)	du (cm)	σe(±cm)	σn(±cm)	σu(±cm)
CK01	120.2104	22.9759	−0.8	0.1	0.9	0.6	0.6	1.0
DONS	120.1537	23.4605	2.1	0.0	0.7	0.6	0.6	1.0
E007	121.5520	23.8255	−30.8	12.6	−15.7	0.9	0.8	6.7
E008	121.6143	23.9930	−29.8	5.5	−16.2	0.9	0.8	7.2
E012	121.4163	23.1251	−16.9	13.1	0.4	0.8	0.8	4.8
E018	120.9100	22.4321	−3.4	−1.1	−4.7	0.8	0.8	6.5
E047	121.3595	23.4707	−21.5	16.3	−11.3	0.8	0.7	4.5
E048	121.4051	23.7095	−35.3	17.9	−5.9	1.0	0.8	8.0
E072	121.2177	23.1529	−7.7	6.3	−11.0	0.9	0.8	6.5
E077	121.5250	23.5964	−30.5	23.6	−12.0	0.8	0.8	5.6
E080	121.0131	23.2202	−5.5	8.7	−1.5	0.8	0.7	4.0
E091	121.4946	24.1826	−20.2	−1.0	−20.2	0.8	0.7	5.4
E300	121.5009	23.5808	−26.6	21.1	−15.4	1.0	1.0	5.4
E302	121.5206	23.9191	−34.1	6.5	−10.7	1.6	1.6	6.4
E307	121.4916	23.8698	−37.6	9.7	10.8	1.6	1.5	9.1
E312	121.5040	23.4832	−22.8	17.5	−17.9	1.3	1.3	8.1
E313	121.4265	23.6753	−36.7	21.7	−13.9	1.4	1.3	9.0
E315	121.5868	23.8877	−29.9	8.0	−6.1	1.3	1.3	6.6
E316	121.4677	23.8157	−34.8	12.8	−11.0	1.5	1.4	8.3
E317	121.4617	23.7214	−31.9	13.8	−7.5	1.1	1.0	7.4
E319	121.6163	24.0500	−24.9	−1.0	−22.3	0.9	0.9	4.6
E323	121.3588	23.3919	−20.8	15.3	−7.6	0.9	0.9	6.4
E324	121.4104	23.4706	−24.2	16.4	−9.1	0.9	0.9	5.7
E328	121.4972	23.6075	−29.3	21.7	−11.9	0.9	0.9	5.7
E333	121.2798	23.1030	−12.7	8.2	−2.2	1.0	0.9	5.7
E340	121.3524	23.4322	−19.4	13.6	−15.9	0.9	0.9	6.0
E341	121.3550	23.3040	−16.7	12.4	−8.4	1.0	1.0	5.2
E349	121.3248	23.3146	−15.8	10.3	−14.7	1.0	1.0	5.4
E361	121.5587	23.7510	−29.6	12.7	−17.2	1.3	1.2	7.6
E363	121.5081	24.2209	−17.3	−2.9	−13.6	1.8	1.8	6.2
E373	121.2880	23.2397	−17.4	11.2	−0.4	1.1	1.1	5.5
E387	121.3272	23.2723	−18.5	12.3	−10.3	1.2	1.2	5.8
E399	121.4950	23.4354	−21.1	15.8	−17.6	1.1	1.1	6.7
E415	121.5730	24.0045	−28.5	1.8	−21.0	1.1	1.0	7.4
E448	121.3994	24.1774	−24.0	1.8	−6.5	1.9	1.9	6.1
E476	121.4343	23.6242	−31.5	20.9	−20.2	1.3	1.2	5.9
E487	121.2571	23.2002	−9.2	4.9	−12.4	1.0	0.9	5.7
E549	121.5405	23.8867	−32.7	7.3	−1.7	1.3	1.3	6.5
E599	121.4914	23.6339	−29.7	21.5	−11.7	1.5	1.5	7.3
E621	121.4462	23.4972	−21.9	15.7	−10.4	1.2	1.3	6.6
E622	121.4027	23.5784	−28.2	21.3	−15.7	1.3	1.3	6.5
E801	121.3183	23.3416	−16.5	11.4	−13.5	1.0	1.0	6.5
E901	121.7694	24.3311	−9.2	−8.0	−19.9	1.0	0.9	6.3
E903	121.3767	23.5335	−25.8	17.2	−16.3	1.0	0.9	6.5
FLNM	121.4533	23.7463	−29.3	13.9	0.8	0.6	0.6	1.0
KDNM	120.7820	21.9494	−1.1	0.6	0.5	0.6	0.6	1.0
KMNM	118.3885	24.4638	0.0	0.0	0.0	—	—	—
M002	120.2167	23.5993	1.4	−2.1	−27.2	0.7	0.7	3.6
M003	120.3093	23.7974	6.1	−3.7	−48.4	0.7	0.7	2.6
M007	120.7744	23.7562	−108.3	71.7	49.6	0.7	0.7	2.7
M031	121.3080	24.3377	−7.7	6.6	−5.3	0.7	0.7	2.9
M036	121.1267	24.0129	−168.1	73.8	−69.8	0.8	0.8	4.8
M043	120.8587	24.1293	−199.2	277.0	135.2	0.7	0.7	2.6
M044	120.5844	24.1381	43.1	−22.8	−2.1	0.7	0.6	2.5
M045	120.6551	24.3563	29.7	−29.2	−0.6	0.7	0.6	2.4
M046	120.7644	24.6013	3.4	−10.1	−9.9	0.7	0.6	2.6
M047	120.9137	24.3672	45.0	−62.9	−39.4	0.7	0.7	2.8
M048	120.8463	24.5560	3.8	−17.5	9.6	1.2	1.3	4.8
M049	120.4461	23.9786	20.6	−8.2	−9.2	0.7	0.7	2.7
M075	120.8488	24.2793	−485.6	702.6	77.6	0.7	0.7	2.9
M081	120.9820	23.9739	−197.0	125.0	−49.0	0.7	0.7	2.7
M083	120.8416	23.9346	−235.2	167.8	74.9	0.8	0.7	4.3
M085	120.6347	23.9276	63.6	−20.9	−9.8	0.7	0.7	2.6
M089	121.2845	24.1524	−51.4	20.3	−33.0	0.7	0.7	3.1
M091	121.1630	24.2512	−14.6	24.2	−2.1	0.7	0.7	2.6
M092	120.3348	23.9536	10.2	−5.3	−13.1	0.9	0.8	6.1
M093	120.4710	23.6938	9.6	−5.1	−0.8	0.7	0.7	2.6
M300	120.4077	24.0204	14.2	−7.6	−8.2	1.0	0.9	3.7
M301	120.8833	24.3915	17.1	−45.9	−7.4	1.3	1.3	6.0
M303	120.9050	23.9951	−207.9	147.7	−8.1	2.2	2.0	10.5
M305	120.8191	23.9982	−306.0	221.8	129.3	2.3	1.8	7.9
M307	120.8442	24.4444	13.5	−31.4	−11.5	1.1	1.0	5.0

Table 3. (continued).

Station	Long. (°)	Lat. (°)	de (cm)	dn (cm)	du (cm)	σe(±cm)	σn(±cm)	σu(±cm)
M309	120.8463	24.1940	−347.8	448.2	158.0	0.9	0.9	3.5
M311	120.9061	24.4676	2.7	−26.5	−1.5	1.1	1.1	5.0
M312	120.8329	24.1713	−328.4	468.7	176.0	1.0	0.9	3.5
M314	120.7499	24.1031	−522.6	499.9	203.8	1.0	0.9	3.3
M315	120.7673	24.2988	60.8	−81.4	−10.5	1.7	1.5	5.7
M316	120.7072	24.0204	−354.0	368.6	269.3	1.3	1.3	4.9
M317	120.4131	23.6350	5.1	−3.8	−7.4	1.0	0.9	3.9
M322	120.7795	23.8370	−277.6	195.2	134.3	2.6	2.4	9.1
M323	121.2696	24.2848	−14.9	11.3	0.4	1.0	0.9	4.3
M324	120.7427	24.2202	−347.4	839.8	401.7	0.8	0.8	3.2
M325	121.0064	24.6442	−1.0	−1.2	1.5	1.6	1.5	6.6
M326	120.5750	24.2542	31.5	−22.3	−3.1	1.0	0.9	3.6
M327	120.6848	24.4938	12.4	−17.0	−12.0	1.0	1.0	4.2
M328	120.8096	24.6271	−0.6	−10.5	1.5	1.4	1.3	5.4
M329	120.6884	24.4434	19.9	−24.5	−6.2	1.0	1.0	4.1
M330	120.8067	24.2245	−350.3	628.2	41.4	1.0	1.0	3.6
M333	120.6320	23.8441	60.5	−20.6	−15.6	1.0	0.9	4.9
M334	120.7518	24.4676	7.1	−17.7	−7.4	0.9	0.9	3.3
M335	120.6098	23.7226	38.4	−10.8	−6.5	1.5	1.4	5.3
M336	120.7600	24.5371	7.7	−14.6	−5.8	1.4	1.4	5.5
M338	120.8930	24.2818	−595.9	631.5	91.7	3.9	3.3	11.3
M340	120.7608	24.5065	10.1	−18.5	−13.4	1.6	1.6	5.5
M341	120.3459	23.7204	4.8	−6.8	−20.2	0.8	0.8	3.4
M343	120.1985	23.5608	−2.1	−2.9	−13.4	0.8	0.8	4.3
M345	120.7525	24.1391	−614.5	645.0	99.8	1.2	1.0	3.8
M346	120.9095	24.6592	0.9	−6.3	−3.7	0.8	0.8	3.3
M349	120.6592	24.2171	56.3	−41.8	3.7	0.9	0.9	3.4
M350	120.7281	24.5012	9.4	−16.1	−10.4	1.3	1.4	9.1
M351	120.5091	23.7845	18.2	−11.1	−5.8	1.0	1.0	3.8
M353	120.6567	24.3078	37.7	−34.6	9.6	0.9	0.9	3.3
M354	120.9484	23.9314	−181.3	123.5	−32.7	2.4	2.0	7.4
M356	120.7952	24.4683	9.6	−24.7	8.1	1.1	1.0	4.3
M357	120.7861	24.4207	19.4	−33.2	−1.0	0.9	0.9	4.8
M358	120.9374	24.5902	0.8	−7.2	−17.9	1.1	1.0	4.9
M359	120.7301	24.3773	30.1	−38.0	−6.9	1.2	1.2	4.8
M360	120.9423	23.8663	−164.7	95.8	−31.7	1.8	1.8	8.6
M361	120.5628	24.1741	36.6	−20.7	3.3	0.8	0.8	2.9
M363	120.6975	24.4173	22.4	−25.0	−5.7	1.1	1.1	4.3
M365	120.6275	23.9839	66.0	−22.1	−14.9	0.9	0.9	3.4
M367	120.6420	23.8200	68.6	−21.4	−18.1	1.0	1.0	4.7
M372	120.5844	23.6597	9.0	−1.3	−20.0	1.7	1.8	5.4
M373	120.5166	24.2223	26.1	−15.5	0.2	0.8	0.8	2.9
M374	120.8557	24.3585	34.9	−64.1	−6.8	1.1	1.1	5.0
M375	120.2263	23.6910	2.8	−3.7	−15.1	1.2	1.2	5.9
M376	120.9952	24.6211	−1.8	−0.9	0.5	1.3	1.2	6.1
M377	120.9035	24.6314	0.3	−5.9	−6.4	1.1	1.0	6.1
M378	120.3045	23.8786	4.6	−3.7	−42.2	1.0	1.0	4.0
M379	120.9513	24.6932	−0.8	−4.5	−4.5	0.9	0.9	3.9
M380	120.8730	24.4875	5.5	−19.9	−7.6	1.0	1.0	3.9
M382	120.9434	24.5035	1.2	3.2	−16.8	1.1	1.0	5.4
M383	120.4779	23.7962	14.4	−6.6	−6.8	1.0	1.0	3.9
M384	120.1883	23.6490	−2.2	−2.2	−9.5	0.9	0.9	4.7
M386	120.7733	24.3803	28.7	−43.1	1.2	1.2	1.2	4.5
M387	120.6496	24.0310	79.0	−33.4	−11.7	0.9	0.9	3.4
M390	120.2257	23.5302	−4.6	−2.7	−13.5	1.0	1.0	4.1
M392	120.3286	23.9040	6.7	−5.2	−43.2	1.1	1.1	4.6
M393	120.7259	24.4589	14.1	−20.3	−10.4	1.1	1.0	5.0
M394	120.6851	24.2613	55.0	−47.9	3.7	2.3	2.5	9.4
M395	120.5856	24.0518	44.5	−19.0	−9.5	1.0	1.0	3.4
M398	120.7120	23.9122	−268.0	17.3	226.4	1.2	1.2	4.8
M400	120.7598	23.6783	−145.4	42.9	44.0	1.3	1.2	5.5
M402	120.9115	24.1015	−253.1	169.4	47.9	1.1	1.0	6.3
M407	120.9143	24.5592	0.9	−10.1	−3.3	1.0	1.0	4.3
M408	120.8491	23.7769	−144.8	83.0	−27.3	1.5	1.2	5.2
M410	120.1837	23.6899	2.3	−2.5	−8.4	0.9	0.9	5.6
M411	120.3220	23.6009	0.8	−2.9	−15.5	1.3	1.2	5.1
M412	120.2851	23.6424	2.4	−3.3	−22.2	1.9	2.1	7.6
M415	120.5644	24.3239	23.9	−21.5	5.9	0.9	1.0	5.0
M416	120.8028	24.1796	−381.1	567.9	101.8	1.0	1.0	3.5
M424	120.5465	23.8222	26.3	−9.1	−12.4	1.1	1.1	4.1
M425	121.2302	24.2241	−33.0	12.8	−14.9	1.0	0.9	4.0
M426	120.9247	24.0470	−218.1	162.8	14.9	1.3	1.2	5.8

Table 3. (continued).

Station	Long. (°)	Lat. (°)	de (cm)	dn (cm)	du (cm)	σe(±cm)	σn(±cm)	σu(±cm)
M427	120.7076	24.5389	7.3	−13.5	−6.7	1.0	0.9	4.4
M428	120.6220	24.3274	30.1	−27.4	3.4	0.8	0.8	3.0
M433	120.7182	23.7350	−40.2	346.0	35.9	1.3	1.3	6.4
M436	120.7135	24.0613	−331.9	283.8	−33.1	1.3	1.3	5.9
M446	120.1666	23.5593	−2.5	−3.5	−13.3	1.5	1.6	11.8
M453	120.4834	24.1525	22.2	−11.0	−2.9	0.9	0.8	3.2
M454	120.5764	23.6306	14.2	2.0	−13.7	1.4	1.4	4.6
M456	120.7854	24.3340	44.7	−65.1	−14.9	1.4	1.3	5.6
M458	120.5881	24.3425	24.8	−20.5	12.5	0.8	0.8	3.4
M459	120.2270	23.7509	6.1	−3.8	−11.2	1.0	0.9	4.8
M461	120.5034	24.0538	27.4	−12.4	−8.5	1.1	1.0	4.0
M467	120.6720	23.9986	97.6	−38.3	−18.4	0.9	0.9	3.5
M473	120.2336	23.7240	2.8	−1.9	−18.9	2.5	2.3	8.7
M474	120.8433	24.2345	−350.1	529.6	125.8	1.2	1.2	4.5
M477	121.3167	24.1871	−29.2	3.2	−11.5	0.9	0.8	3.9
M478	120.6402	23.7704	57.6	−15.1	−9.3	1.4	1.4	5.0
M479	120.7158	23.8436	−321.9	97.9	256.7	1.1	1.0	5.3
M482	120.7006	23.9666	−372.9	347.8	332.6	1.0	1.0	4.8
M486	120.4749	24.0902	25.6	−12.2	−2.9	0.8	0.8	3.0
M487	121.2315	24.1165	−86.9	43.3	−59.7	1.4	1.4	5.6
M491	121.2006	24.1514	−79.2	25.8	−16.0	1.8	1.9	5.6
M493	120.7199	23.7754	−249.9	−55.3	109.5	1.5	1.3	6.1
M494	121.1647	24.1611	−82.5	27.1	−21.2	1.4	1.4	4.8
M501	120.9082	23.9512	−193.8	140.8	4.4	1.0	1.0	4.5
M507	120.8628	23.7243	−155.8	82.7	−38.8	0.9	0.8	3.8
M509	120.8981	23.8140	−161.8	74.1	−42.4	1.2	1.1	5.9
M514	120.4416	23.8673	13.8	−7.7	−13.2	1.0	1.0	4.0
M527	120.7653	23.8935	−262.7	376.9	119.9	1.0	1.0	4.3
M533	120.2604	23.6973	0.9	−3.4	−19.6	1.6	1.5	6.3
M553	120.2781	23.6106	1.3	−1.7	−21.4	2.5	2.3	8.1
M554	120.4244	23.6828	7.2	−4.7	−8.6	1.2	1.2	4.5
M561	120.4172	23.8170	10.3	−6.8	−18.6	2.1	2.0	7.2
M573	120.4174	23.7828	10.2	−5.5	−3.3	1.0	1.0	3.9
M574	120.3269	23.6816	1.2	−5.0	−25.7	1.2	1.2	4.6
M581	120.9405	24.2291	−274.2	226.6	116.3	1.9	1.8	6.0
M584	120.9711	24.2104	−62.6	71.7	211.3	1.8	1.7	5.3
M586	120.6610	23.8825	71.8	−26.6	−15.4	1.0	1.0	4.9
M587	120.8977	24.2187	−287.6	455.1	32.4	1.6	1.6	5.2
M593	121.2253	24.1917	−52.1	19.8	−18.1	1.0	1.0	4.1
M599	121.1930	24.2508	−23.4	19.0	−18.5	1.0	0.9	4.3
M601	120.7516	24.0028	−378.1	337.0	323.8	1.2	1.2	4.8
M614	120.6315	23.8892	58.7	−19.7	−20.4	1.0	0.9	5.2
M674	120.1435	23.6340	0.7	−1.7	−7.5	1.1	1.0	6.0
M694	120.5784	23.5834	−2.2	−3.0	−4.0	1.2	1.2	6.9
M714	120.8340	24.3245	47.1	−77.6	−10.9	1.8	1.8	6.6
M801	120.8754	24.6840	0.0	−5.3	−2.4	0.9	0.9	3.8
M802	120.8183	24.5619	3.0	−12.8	−9.1	0.9	0.9	4.3
M804	120.7140	24.2491	66.4	−60.1	−4.1	0.8	0.8	3.4
M805	120.6805	24.1708	74.5	−48.1	3.7	0.8	0.8	3.2
M806	120.6533	24.1537	64.2	−39.2	−6.2	0.8	0.8	3.0
M807	120.4982	24.1172	25.2	−13.3	−3.5	0.8	0.8	3.0
M808	120.6856	24.1106	89.6	−51.2	−11.0	0.9	0.9	3.2
M809	120.4355	24.0571	19.4	−9.1	−1.0	1.0	1.0	3.4
M810	120.5800	23.9627	43.8	−12.6	−18.3	0.9	0.9	3.3
M811	120.4746	23.9612	17.2	−10.3	−17.3	0.8	0.8	3.3
M812	120.3734	23.8999	9.1	−6.7	−40.7	1.5	1.1	4.8
M813	120.5247	23.8749	24.7	−7.5	−15.3	0.8	0.8	3.4
M814	120.5814	23.8645	38.7	−13.7	−14.7	0.9	0.9	4.0
M816	120.4448	23.7080	9.3	−4.3	−9.9	0.8	0.8	3.5
M901	120.8719	24.7146	−1.3	−3.4	−7.3	1.1	1.1	4.5
M902	120.9301	24.4512	8.8	−16.9	−2.1	1.6	1.7	6.8
M903	120.6059	24.4158	19.5	−18.2	−10.6	0.8	0.8	3.0
M904	120.6067	24.2985	34.0	−26.7	6.0	0.8	0.8	3.1
M905	121.2570	24.2534	−17.8	9.2	−6.3	1.0	1.0	5.1
M906	120.5223	24.2562	23.7	−18.0	1.5	1.0	1.0	3.6
M907	120.6327	24.0677	62.4	−29.8	−6.9	0.9	0.9	3.2
M908	120.5193	24.0155	27.6	−12.3	−11.3	1.0	1.0	3.5
M909	120.4409	24.0095	16.7	−8.4	−10.2	0.9	0.9	3.5
M910	120.4137	23.9564	11.9	−5.4	−15.7	1.0	0.9	3.6
M911	120.4245	23.8929	14.4	−6.8	−8.5	0.8	0.8	3.4
M912	120.9332	23.7754	−152.2	80.5	−47.4	0.9	0.9	4.2
M913	120.9425	24.0175	−200.2	145.8	−36.2	1.3	1.2	5.9

Table 3. (continued).

Station	Long. (°)	Lat. (°)	de (cm)	dn (cm)	du (cm)	σe(±cm)	σn(±cm)	σu(±cm)
M914	120.3776	23.7581	7.6	−7.1	−14.0	1.0	1.0	3.8
M915	120.8201	24.5230	6.7	−17.3	−12.8	1.0	1.0	3.8
M916	120.7119	24.3315	39.1	−41.8	−5.4	1.0	1.0	3.5
M917	120.6313	24.1744	54.6	−33.7	−3.1	0.8	0.8	3.1
M918	120.5070	23.9531	23.6	−8.9	−22.3	0.8	0.8	3.1
M938	121.1717	24.0807	−118.1	36.9	−30.2	1.7	1.7	5.5
M959	121.1823	24.0291	−118.9	15.7	−43.5	1.3	1.3	4.6
M961	121.1319	23.9798	−130.1	27.0	−55.5	1.2	1.2	4.7
M999	120.8612	23.9717	−231.8	184.3	55.2	1.5	1.4	9.2
MZUM	119.9331	26.1571	−0.4	−0.1	0.6	0.6	0.6	1.0
N011	121.2915	25.1025	0.0	0.3	−10.6	0.7	0.7	4.3
N023	121.0500	24.6804	−2.6	0.8	−2.4	0.7	0.7	3.4
N028	120.9439	24.7857	−1.2	−1.4	3.6	0.7	0.7	3.0
N032	121.1139	24.5065	−6.1	11.0	−20.1	0.7	0.7	2.6
N052	121.8678	24.5939	2.8	−5.3	−12.7	0.7	0.7	4.8
N053	121.7779	24.3973	−3.4	−8.9	−14.5	0.7	0.7	4.6
N090	121.6189	24.6592	0.5	−0.2	−7.3	0.7	0.7	4.7
N091	121.2521	25.0015	0.5	−0.1	−11.7	0.7	0.7	4.6
PKGB	120.3051	23.5796	1.5	−1.7	−5.9	2.8	3.4	9.4
PKGM	120.3054	23.5799	4.3	−0.3	0.2	0.6	0.6	1.0
S003	120.1627	23.1731	−4.1	−1.4	−9.2	0.7	0.7	4.3
S020	120.6231	23.5900	−21.9	−35.1	−55.1	0.8	0.7	4.6
S021	120.4807	23.5358	−0.8	−3.3	−2.9	0.7	0.7	3.7
S023	120.1887	23.3825	−2.4	−4.1	−33.0	0.7	0.7	2.9
S025	120.8244	23.2636	−7.5	−0.7	2.4	0.7	0.7	3.6
S026	120.9572	23.4700	−33.8	21.5	−17.5	0.7	0.7	3.3
S027	120.8895	23.4838	−34.0	26.9	−11.3	0.7	0.7	3.3
S031	119.5690	23.5291	−3.4	−0.3	−1.6	0.8	0.7	4.8
S034	120.3817	22.5301	−4.6	−4.6	−8.7	1.0	1.0	8.9
S059	120.5081	23.1945	−8.6	−2.9	−0.4	0.8	0.8	5.6
S070	120.5620	23.4520	−8.4	−6.3	3.2	0.7	0.7	3.0
S091	120.3124	23.3383	−4.2	−4.5	−24.3	0.7	0.7	3.9
S092	120.2904	23.4515	−1.7	−3.7	−7.9	0.7	0.7	3.4
S313	120.5636	23.2536	−28.4	−15.4	8.2	1.4	1.4	5.0
S317	120.5822	23.3004	−8.3	−6.2	9.7	1.3	1.2	5.3
S322	120.2962	23.4819	0.4	−3.3	−35.1	1.0	0.9	4.6
S326	120.6949	23.4701	−13.3	−8.6	−5.7	1.1	1.0	4.6
S328	120.6080	23.5672	−13.0	−16.1	−9.4	0.9	0.9	6.0
S330	120.7100	23.5622	−13.0	−14.0	−10.2	1.2	1.2	4.3
S338	120.4086	23.5991	4.7	−3.1	−5.4	1.0	1.0	5.1
S344	120.3471	23.5320	−1.0	−2.6	−7.1	1.2	1.1	4.9
S346	120.1930	23.2924	−6.0	−1.7	−30.3	1.0	1.0	4.7
S349	120.3038	23.3936	−3.9	−4.6	−21.1	0.9	0.9	3.9
S358	120.3940	23.5145	−2.3	−4.5	−0.7	1.3	1.2	6.5
S371	120.3219	23.4694	−0.7	−5.1	−5.8	1.0	0.9	5.3
S377	120.5251	23.4056	−7.1	−7.7	4.7	2.1	2.1	8.3
S378	120.3639	23.5646	0.3	−3.7	−7.0	1.1	1.0	4.4
S384	120.1553	23.4696	−6.0	−9.5	−8.9	1.1	1.2	4.8
S388	120.5975	23.3462	−21.8	−12.3	−22.9	2.0	2.0	7.2
S390	120.5665	23.4118	−6.3	−4.9	4.2	2.2	2.1	7.9
S391	120.5197	23.5824	1.3	−2.7	−6.8	1.6	1.3	5.5
S396	120.4919	23.4800	−1.1	−2.1	−14.6	3.3	3.3	10.7
S405	120.2754	23.4178	−3.4	−4.5	−11.6	0.9	0.8	3.9
S414	120.6487	23.4044	−9.4	−8.7	10.2	1.2	1.1	5.7
S417	120.2299	23.4109	−4.7	−3.6	−10.1	1.2	1.2	4.6
S421	120.6038	23.4590	−8.8	−9.7	−4.8	1.0	1.0	6.3
S426	120.9163	23.2822	−9.3	4.2	−7.4	1.0	1.0	4.4
S434	120.2310	23.4509	−5.0	−3.9	−10.5	1.2	1.2	4.4
S465	120.4222	23.4600	−2.3	−5.5	−4.9	1.3	1.2	5.0
S608	120.4436	23.4201	−3.7	−5.8	4.8	1.0	1.0	3.8
S690	120.6579	23.4370	−6.4	−6.3	6.3	1.1	1.0	4.6
S801	120.4583	23.6005	4.7	−2.6	−6.9	1.0	0.9	3.9
S802	120.5474	23.5135	−4.1	−4.7	−4.1	0.9	0.8	3.9
S803	120.3957	23.4335	−3.7	−6.2	−9.4	1.2	1.1	4.7
S901	120.3611	23.5955	−0.9	−3.1	−21.6	1.0	1.0	4.1
S902	120.1904	23.4991	−5.5	−1.0	−7.2	1.0	1.0	4.9
S903	120.1819	23.4367	−6.2	−3.0	−20.2	1.1	1.2	4.4
TMAM	121.0074	22.6161	−1.6	1.7	0.1	0.6	0.6	1.1
YMSM	121.5740	25.1657	0.0	0.4	0.7	0.6	0.6	1.0

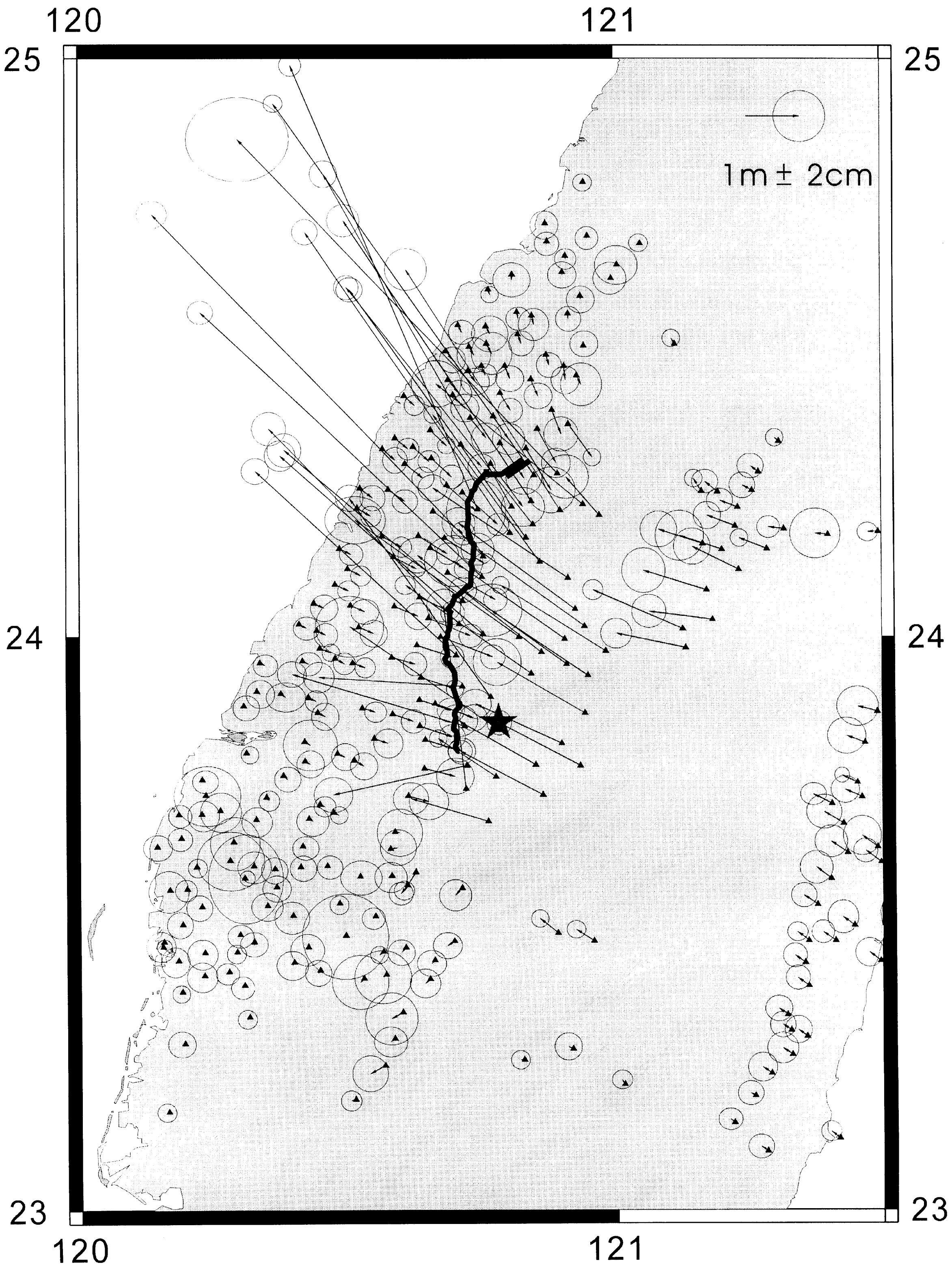

Fig. 5(a). Measured horizontal displacements associated with the Chi-Chi earthquake, where the main shock is shown as a star and station locations are indicated by triangles. Surface rupture is indicated by a thick line. Displacement of a single station is shown by a vector and corresponding 1-sigma error ellipse.

Goad and Yang, 1997; Yang and Lo, 2000). Since high-precision orbits of the GPS satellites could be obtained from IGS data centers with an estimated coordinate RMS of 5–10 cm (Neilan *et al.*, 1997; Beutler *et al.*, 1999), in this study we used fixed IGS precise ephemeris. To remove the first-order ionospheric effect, the so-called ionosphere-free phase combination was formed (Beutler *et al.*, 1996). The modified Hopfield model (Goad and Goodman, 1974) was used to give the nominal tropospheric delays on GPS phase measurements. Additionally, one correction parameter per station every 4 hours was estimated to absorb unmodelled tropospheric errors. A summary of our data reduction strategy is given in Table 1. We primarily used the Bernese 4.0 software, developed at the University of Berne, Switzerland, as our fundamental tool for GPS data analysis (Beutler *et al.*, 1996).

The network adjustment was carried out in two steps. In the first step only data in the first group, i.e., daily measurements from the global and regional tracking networks, were analyzed. The coordinates and velocities of the IGS stations were stochastically constrained to their *a priori* values defined in the ITRF94, with the associated coordinate and velocity standard deviations defined in the same frame (Boucher *et al.*, 1996). Given the high data density and sufficient elapse time, reliable coordinate and velocity estimates defined in the ITRF94 at epoch 1997.0 (approximately the mid-point of the data span) for the regional tracking stations were determined (Yang *et al.*, 1999). The resultant millimeter-level coordinate and velocity standard deviations for the regional tracking stations are summarized in Table 2.

The coordinates of the 726 first- and second-order control stations were determined in the second step, where only the GPS data in the second group were analyzed. The stochastic information regarding the regional tracking stations obtained from the first step, i.e., the ITRF94 velocities and coordinates and their associated standard deviations listed in Table 2, was applied in the second step. The coordinate variation rates of the first- and second-order stations, however, were not estimated, as the number of occupations per station was not sufficient for us to recover reliable velocity information.

The resultant 1997.0 TWD97 station coordinates, including the regional tracking stations, were measured with accuracies ranging from 0.1 to 3.0 cm in the east-west and north-south directions, and 0.1 to 9.7 cm in the vertical direction for most stations. The precision of the vertical component was noticeably worse than that of the horizontal components for the 726 first- and second-order points, which was mainly caused by the insufficient length of observation sessions (only 4–5 hr) for effective decorrelation of the vertical component with other error sources (Beutler *et al.*, 1989; Kuang *et al.*, 1996; Yang *et al.*, 1999).

The collection of post-earthquake data at the TWD97 first- and second-order stations located in the central Taiwan area was completed within one month of the devastating event. Each station was occupied at least twice with field sessions of 4–5 hr in length. The data were then combined with continuously recorded regional tracking data covering 24 hours on the day of each observation session. To identify seismic effects associated with the earthquake on the regional tracking stations, we examined several long baselines connecting

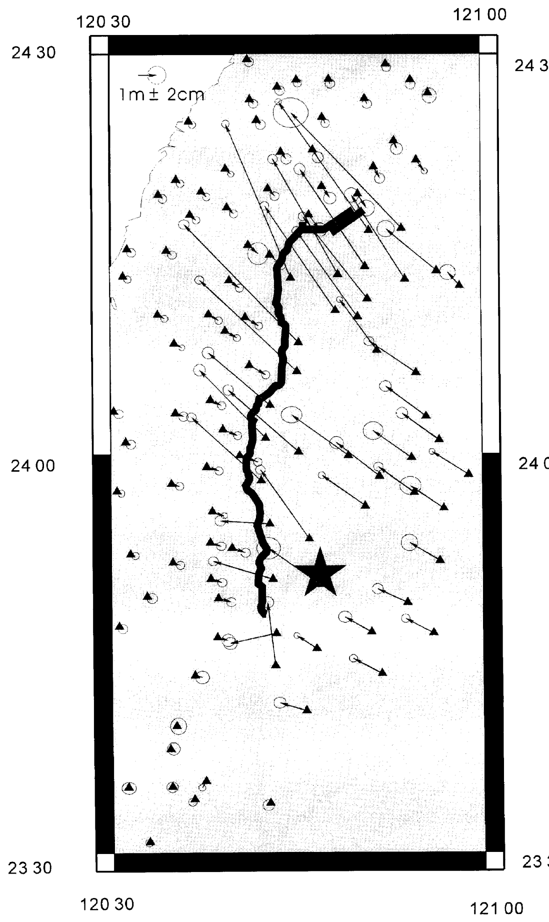

Fig. 5(b). Measured horizontal displacements associated with the Chi-Chi earthquake (near field).

the distant IGS site GUAM with the regional tracking stations for a period of 80 days (day 230–309). Two distinct cases are discussed here. Figure 3 displays the daily solutions of baseline length ($\sim$2688 km) for the GUAM-FLNM (located in the east coast of Taiwan Island) baseline. The earthquake occurred at 17:47 on day 263 (GMT), therefore the solution for that day was obtained using only data collected prior to the epoch. FLNM experienced an apparent co-seismic motion of the order of 30 centimeters, the largest among all continuous tracking stations. Nevertheless, no evidence of pre- or post-seismic motions can be definitely identified in Fig. 3. Figure 4 shows the daily solutions of baseline length ($\sim$3000 km) for the GUAM-KMNM (located on Kinman Island across Taiwan Strait) baseline. A secular decrease in the distance due to tectonic convergence can be observed from Fig. 4; however, different from the previous case, in this line we cannot positively single out any seismic signals associated with the earthquake.

To compute the post-earthquake coordinates of the TWD97 stations, again we adopted the same data processing strategy listed in Table 1. In the network adjustment, we only minimally constrained the position of the KMNM tracking station, where no definite seismic motion is detected (see Fig. 4). To accommodate secular crustal movements between the reference epoch at 1 January 1997 (1997.0) and

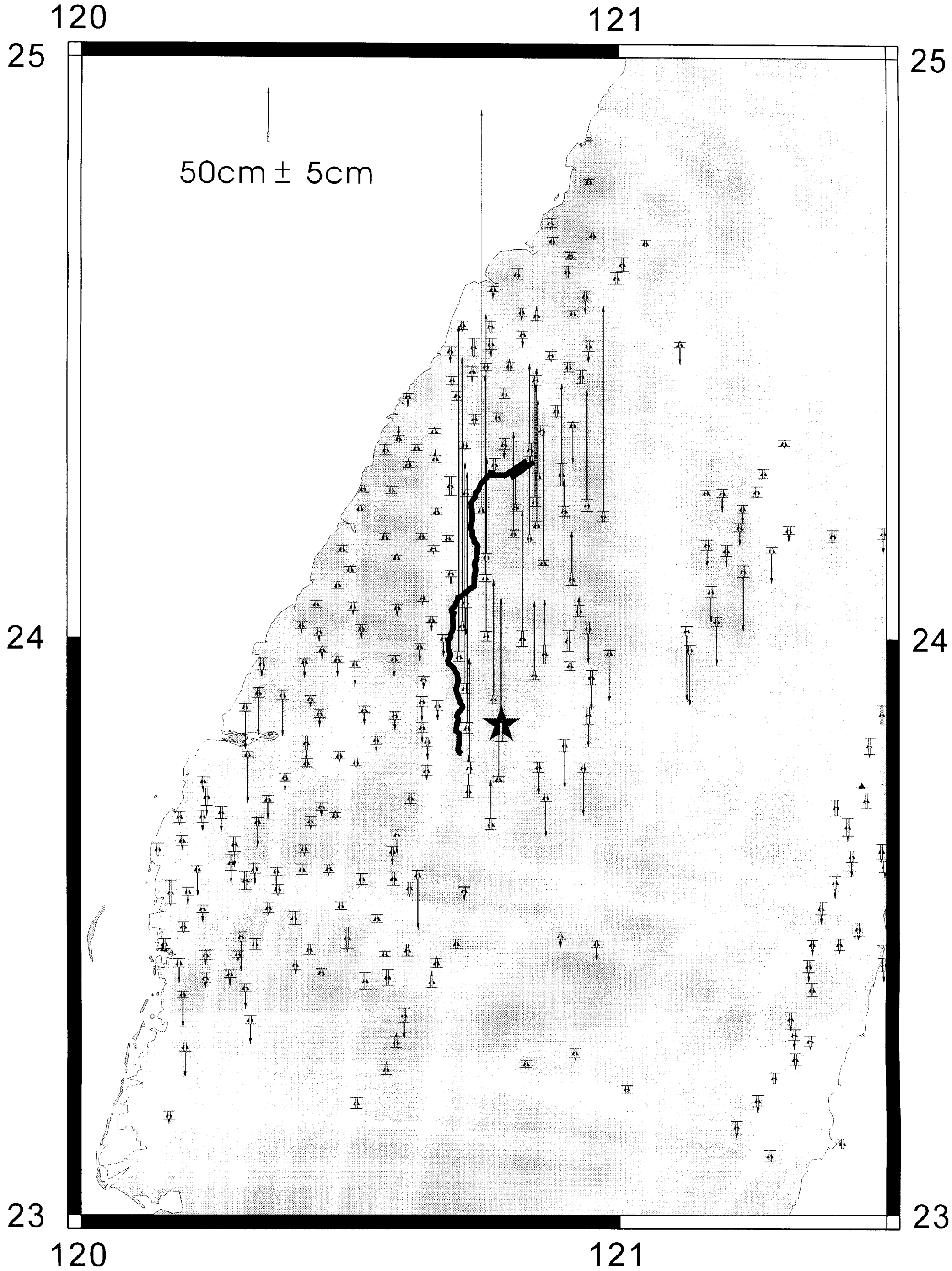

Fig. 6. Measured vertical displacements associated with the Chi-Chi earthquake, where the main shock is shown as a star and station locations are indicated by triangles. Surface rupture is indicated by a thick line. Displacement of a single station is shown by a vector and corresponding 1-sigma error bar.

the earthquake epoch at 21 September 1999, annual station velocities for the TWD97 stations were interpolated from the velocity field given in Fig. 1 (Yu *et al.*, 1997). Since the relative inter-seismic motions for the sampled stations are well known, there is little error introduced by interpolating these motions. The final surface displacement field is sampled at 285 GPS-derived vectors measured with 1-sigma errors ranging from 0.6 to 3.9 cm in the east-west direction, 0.6 to 3.4 cm in the north-south direction, and 1.0 to 11.8 cm in the vertical direction. The final displacement vectors and their associated sigma values are presented in Table 3.

3. Analysis

Figures 5(a), 5(b) and 6 illustrate the spatial distribution of the horizontal and vertical co-seismic displacement vectors. In the figures, the thick black line indicates the surface rupture produced by the earthquake and the epicenter is shown as a large star near the southern end of the rupture zone. The relative motion direction between GPS sites across the fault is northwestward in general, which is consistent with the relative motion of the Philippine Sea plate. The surface rupture extends for about 75 km along the north-south trending Chelungpu fault, but at the northern end of the fault, the rupture extends towards the northeast for an additional 10 km in a major sub-event and splinters into complex branches (Ma *et al.*, 1999). Individual GPS stations within 15 km east of the fault (the hanging-wall) generally are uplifted by 0.2–4 m and displaced northwestward by 1.5–9 m. The largest horizontal and vertical offsets are placed at the northern end of the ruptured Chelungpu fault. The GPS stations situated further to the east of the rupture zone all the way to the east coast generally are subsided by up to 0.8 m, and displaced northwestward by 0.1–3 m. To the west of the fault (the footwall), in general, individual stations are subsided by up to 0.5 m and displaced southeastward by up to 1.2 m. It is also interesting to note that after the earthquake liquefaction-related ground failures have been reported in regions near the western coastline, which can be identified with the erratically large subsidence quantities up to 0.5 m in the corresponding area (see Fig. 6).

4. Conclusion

Damaging earthquakes have previously occurred in western Taiwan several times this century: in 1904 (Tou-Liu $M = 6.1$), 1906 (Mei-Shan $M = 7.1$), 1916–17 (Nan-Tou $M = 6.8$), 1935 (Hsin-Chu Tai-Chun $M = 7.1$), 1941 (Chung-Pu $M = 7.1$), 1946 (Hsin-Hua $M = 6.1$), and 1964 (Bai-Ho $M = 6.3$). Although several of these earthquakes produced vertical slips of the order of 1 m (Cheng *et al.*, 1999), none has released as much seismic energy as the Chi-Chi earthquake. As Taiwan's strongest earthquake of the century, this $M_w = 7.6$ earthquake has produced spectacular surface ruptures among the largest fault movements ever observed from modern earthquakes (Ma *et al.*, 1999).

The co-seismic displacements of the Chi-Chi earthquake were accurately determined in this study with geodetic data recorded by the dense Taiwanese GPS network before and after the earthquake. This paper describes the collection and analysis of the GPS data, and creates a comprehensive data set for the displacement field. The abundant information contained in the data set could be further inverted to determine the rupture geometry and slip distribution associated with the Chi-Chi earthquake in future geophysical studies.

Acknowledgments. The authors are grateful to the Ministry of the Interior, R.O.C. for financially supporting this research and to the Bureau of Land Survey, R.O.C. for its contribution in the collection of post-earthquake GPS data. We specially thank Dr. Kosuke Heki and Dr. Zheng-Kang Shen for their important suggestions and constructive criticism.

References

Beutler, G., I. Bauersima, B. Botton, W. Gurtner, M. Rothacher, and T. Schildknecht, Accuracy and biases in the geodetic application of the Global Positioning System, *Manuscr. Geod.*, **14**, 28–35, 1989.

Beutler, G., E. Brockmann, S. Fankhauser, W. Gurtner, J. Johnson, L. Mervart, M. Rothacher, S. Schaer, T. Springer, and R. Weber, *Bernese GPS Software Version 4.0*, University of Berne, Berne, Switzerland, 1996.

Beutler, M. Rothacher, S. Schaer, T. Springer, J. Kouba, and R. E. Neilan, The international GPS service (IGS): an interdisciplinary service in support of earth sciences, *Adv. Space Res.*, **23**, 631–653, 1999.

Boucher, C., Z. Altamimi, M. Feissel, and P. Sillard, Results and analysis of the ITRF94, IERS Technical Note 20, 206 pp., Observatoire de Paris, Paris, France, 1996.

Cheng, S.-N, Y.-T. Yeh, M.-T. Hsu, and T.-C. Shih, Photo album of ten disastrous earthquakes in Taiwan, CWB-9-1999-002-9, Central Weather Bureau and the Institute of Earth Sciences, Academia Sinica, Taiwan, R.O.C., 289 pp., 1999.

DeMets, C., R. G. Gordon, D. F. Argus, and S. Stein, Current plate motions, *Geophys. J. Int.*, **101**, 425–478, 1990.

Goad, C. C. and L. Goodman, A modified Hopfield tropospheric refraction correction model, Fall Annual Meeting of the Amer. Geophys. U., San Francisco, CA, U.S.A., Dec. 12–17, 1974.

Goad, C. C. and M. Yang, A new approach to precision airborne GPS positioning for photogrammetry, *Photogrammetric Eng. & Remote Sensing*, **63**, 1067–1077, 1997.

Goad, C. C., D. A. G.-Brzezinska, and M. Yang, Determination of high-precision GPS orbits using triple differencing technique, *J. Geod.*, **70**, 655–662, 1996.

Kuang, D., B. E. Schutz, and M. M. Watkins, On the structure of geometric positioning in GPS measurements, *J. Geod.*, **71**, 35–43, 1996.

Ma, K.-F., C.-T. Lee, and Y.-B. Tsai, The Chi-Chi, Taiwan earthquake: large surface displacements on an island thrust fault, *Eos Trans. AGU*, **80**, 608–611, 1999.

Neilan, R. E., J. F. Zumberge, G. Beutler, and J. Kouba, The international GPS service: a global resource for GPS applications and research, in *Proc. ION GPS-97*, Sept. 16–19, Kansas City, MO, U.S.A., pp. 883–889, 1997.

Seno, T., S. Stein, and A. E. Gripp, A model for the motion of the Philippine Sea Plate consistent with NUVEL-1 and geological data, *J. Geophys. Res.*, **98**(B10), 17,941–17,948, 1993.

Yang, M. and C. F. Lo, Real-time kinematic GPS positioning for centimeter level ocean surface monitoring, *Proc. Natl. Sci. Counc. ROC(A)*, **24**, 79–85, 2000.

Yang, M., C.-L. Tseng, J.-Y. Yu, and K.-H. Chen, Adjustment and accuracy analysis of Taiwan first-order GPS control network, *J. Cadastral Surv.*, **18**(2), 1–27, 1999 (in Chinese).

Yu, S.-B., H.-Y. Chen, and L.-C. Kuo, Velocity field of GPS stations in the Taiwan area, *Tectonophys.*, **274**, 41–59, 1997.

Yu, S.-B., L.-C. Kuo, R. S. Punongbayan, and E. G. Ramos, GPS observation of crustal deformation in the Taiwan-Luzon region, *Geophys. Res. Lett.*, **26**, 923–926, 1999.

M. Yang (e-mail: myang@mail.ncku.edu.tw)